

Localization threshold of Instantaneous Normal Modes from level-spacing statistics

Stefano Ciliberti¹ and Tomás S. Grigera²

¹*Departamento de Física Teórica I, Universidad Complutense de Madrid, Madrid 28040, Spain*

²*Instituto de Investigaciones Fisicoquímicas Teóricas y Aplicadas (INIFTA, CONICET-UNLP), c.c. 16, suc. 4, 1900 La Plata, Argentina.*

We study the statistics of level-spacing of Instantaneous Normal Modes in a supercooled liquid. A detailed analysis allows to determine the mobility edge separating extended and localized modes in the negative tail of the density of states. We find that at temperature below the mode coupling temperature only a very small fraction of negative eigenmodes are localized.

PACS numbers: 61.43.Fs, 63.50.+x

I. INTRODUCTION

The Instantaneous Normal Modes (INM) of a liquid are the eigenvectors of the Hessian (second derivative) matrix of the potential energy, evaluated at an instantaneous configuration. The interest in the equilibrium-average properties of the INM originates in the proposal [1] to use them to study liquid dynamical properties, especially diffusion, which is considered to be linked to unstable modes (a subset of the modes with negative eigenvalue) [2, 3, 4, 5, 6, 7]. They have been naturally applied to address the problem of the glass transition: the glass phase is viewed as that where free (*i.e.* non-activated) diffusion is absent, and the disappearance of diffusion should be linked to that of the unstable modes [2]. The identification of these unstable modes presents some problems [8, 9], and the localization properties of the INM are of interest. This is the problem we address here.

Localization is an interesting and difficult problem in its own right. Given an $N \times N$ random matrix defined by the probability distribution of its elements in some (typically site) base, the problem is to determine whether an eigenmode projects to an extensive number of base vectors (extended state) or not (localized state) in the large N limit. Only in a few cases there is a theoretical solution for this problem [10, 11, 12]. From the point of view of random matrix theory, the INM are the eigenvectors of an Euclidean random matrix (ERM) [13], and the problem of localization in ERMs has been recently addressed analytically in the dilute limit [14]. Clearly, the problem is also hard from the numerical point of view, involving a question about the thermodynamic limit. Quantities such as the participation ratio [15], which can distinguish between localized and extended states but require knowledge of the eigenvectors, are problematic numerically because computation of eigenvectors is very expensive for large systems.

Here we explore an approach [16] relying only on eigenvalues, based on the fact that the statistics of level spacing is strongly correlated with the nature of the eigenmodes (see sec. II). We apply it for the first time to a model glass-forming liquid at a temperature below the mode coupling temperature T_c [17]. Our work can be regarded as an extension of the results of ref. 6, as far as we

perform a detailed analysis of the level spacing. Our emphasis is on the exploring the usefulness of level-spacing statistics as a means to obtain a localization threshold in off-lattice systems and the possible limitations of this technique.

II. THEORETICAL BACKGROUND

The spectral function of the eigenvalues of a random matrix is $S(\lambda) = \sum_i \delta(\lambda - \lambda_i)/N$. Its (disorder-) average is the density of states $g(\lambda)$ (DOS). The cumulative spectral function for this particular realization of the disorder,

$$\eta(\lambda) = \int_{-\infty}^{\lambda} d\lambda' S(\lambda') = \frac{1}{N} \sum_{i=1}^N \theta(\lambda - \lambda_i), \quad (1)$$

can be decomposed into a smooth part plus a fluctuating term $\eta_{\text{fluct}}(\lambda)$, whose average is zero. The smooth part is then

$$\zeta(\lambda) \equiv \langle \eta(\lambda) \rangle = \int_{-\infty}^{\lambda} d\lambda' g(\lambda'). \quad (2)$$

The level spacing is not studied directly on the λ_i , because it depends on the mean level density. To eliminate this dependence, one “unfolds” the spectrum, which means to map the original sequence $\{\lambda_i\}$ onto a new one $\{\zeta_i(\lambda_i)\}$ according to Eq. (2) (see *e.g.* [18] for a detailed explanation of this point). The cumulative spectral function can be expressed in terms of these new variables:

$$\hat{\eta}(\zeta) \equiv \eta(\lambda(\zeta)) = \zeta + \hat{\eta}_{\text{fluct}}(\zeta). \quad (3)$$

The distribution of the variable ζ is uniform in the interval $[0, 1]$ regardless the $g(\lambda)$.

The nearest-neighbor spacing distribution $P(s)$ gives the probability that two *neighboring* unfolded eigenvalues ζ_i and ζ_{i+1} are separated by s . It is one of the most commonly used observables in random matrix theory. It is different from the two level correlation function and it involves all the k -level correlation functions with $k \geq 2$ [19]. It displays a high degree of universality, exhibiting common properties in systems with very different spectra. Although no general proof has been given, its shape

is thought to depend only on the localization properties of the states [18]. In the case of the Gaussian Orthogonal Ensemble (GOE), where all states are extended in the thermodynamic limit, it is known [19] that $P(s)$, normalized such that $\langle s \rangle = 1$, follows the so-called *Wigner surmise* (also known as Wigner-Dyson statistics), namely

$$P_{\text{WD}}(s) = \frac{\pi s}{2} \exp(-\pi s^2/4). \quad (4)$$

The linear behavior for small s is an expression of the level repulsion. This form actually characterizes many different systems with extended eigenstates (see e.g. ref. 20 and references therein). In the case of INM, it has been shown [6] that it describes the level spacing better and better as the fraction of localized states decreases.

On the other hand, a system whose states are all localized will have completely uncorrelated eigenvalues. This corresponds to a Poisson process, and the statistics of two adjacent levels is given by

$$P_{\text{P}}(s) = \exp(-s). \quad (5)$$

If one deals with a set of levels which includes both localized and extended states, one expects some distribution interpolating between those two. A natural ansatz is the simple linear combination

$$P_{\text{LC}}(s; \pi) = (1 - \pi)P_{\text{P}}(s) + \pi P_{\text{WD}}(s), \quad (6)$$

which holds under the hypothesis that contributions coming from localized and extended modes simply add linearly. Another possibility comes from a statistical argument due to Wigner (see for example [19]), that leads to the heuristic function

$$P(s) = \mu(s) \exp \left\{ - \int_0^s ds' \mu(s') \right\}, \quad (7)$$

where $\mu(s)$ is called *level repulsion function*. Taking $\mu(s) = c_q s^q$, with $q \in [0, 1]$, one obtains the Brody distribution [21]

$$P_{\text{B}}(s; q) = c_q s^q \exp \left(- \frac{c_q s^{q+1}}{q+1} \right), \quad c_q = \frac{\Gamma^{q+1}[1/(q+1)]}{q+1}, \quad (8)$$

which interpolates between the Poisson ($q = 0$) and Wigner-Dyson ($q = 1$) distributions. However, this is just another phenomenological interpolation scheme, since there is no theoretical argument supporting a level repulsion function increasing as a power law with an exponent smaller than one.

III. METHOD

The practical difficulty in performing the unfolding lies in finding a good approximation to the smooth (averaged) part of the cumulative spectral function, $\zeta(\lambda)$. We

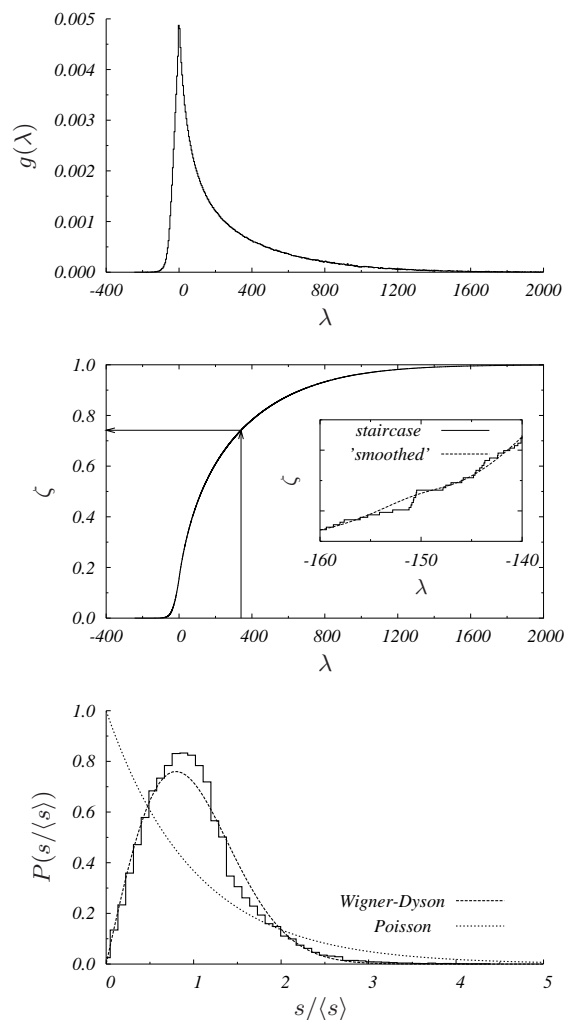


FIG. 1: Evaluation of the level-spacing statistics. Top: INM spectrum of unit density soft-sphere (pair potential $1/r^{12}$) system at $T = 0.68$, as obtained from the numerical diagonalization of 100 thermalized configurations. Middle: The cumulative function of the same system and decomposition in *smooth* and *fluctuating* parts (inset). Bottom: The level-spacing distribution of this system, normalized to have $\langle s \rangle = 1$. Poisson and Wigner-Dyson distributions are also shown for comparison.

have first obtained a cumulative function averaged over many samples of the Hessian (computed from a corresponding number of equilibrium configurations) and then taken $\zeta(\lambda)$ as the function defined by a cubic spline interpolation of the resulting staircase. Once this function is defined, the spacings of each sample can be evaluated by extracting the λ values according to the $g(\lambda)$ and then computing $s = \zeta(\lambda_{i+1}) - \zeta(\lambda_i)$; the histogram of these values is an estimate of the $P(s)$. We have also tried digital filtering (Savitsky-Golay [23]) of the staircase, but the results were not satisfactory. The procedure is illustrated in Fig. 1.

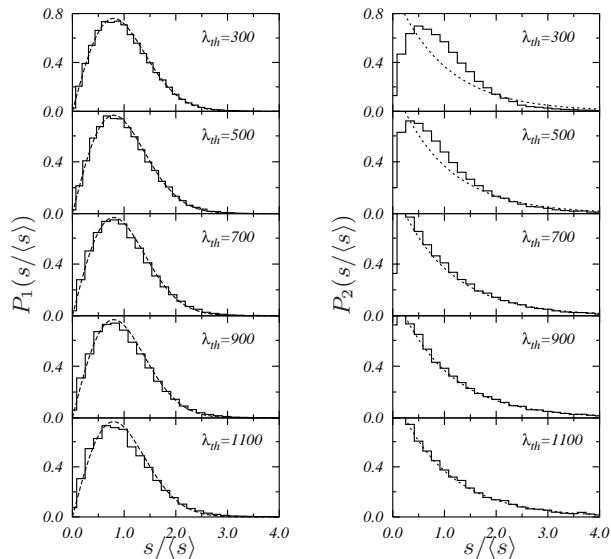


FIG. 2: Level spacing distributions $P_1(s/\langle s \rangle)$ and $P_2(s/\langle s \rangle)$ obtained from the positive part of the spectrum of Fig. 1 for several values of λ_{th} . Wigner-Dyson (left) and Poisson (right) distributions are also plotted.

To estimate the localization threshold λ_L , we proceed as follows. We divide the full spectrum into two parts at an arbitrary threshold λ_{th} and study (after proper unfolding) the restricted level-spacing distributions $P_1(s) \equiv P(s|\lambda < \lambda_{th})$ and $P_2(s) \equiv P(s|\lambda > \lambda_{th})$. The localization threshold (where it exists) should correspond the value of λ_{th} that leads to $P_1(s) = P_{WD}(s)$ (extended eigenstates) and $P_2(s) = P_P(s)$ (localized eigenstates). On the other hand if $\lambda_{th} \neq \lambda_L$, $P_1(s)$ and $P_2(s)$ will bear more similarity to each other, since one of them will include spacings from both localized and extended levels. A qualitative feeling of what happens as λ_{th} moves through the spectrum can be gathered from Fig. 2, where it can be clearly seen how $P_2(s)$ evolves from a nearly Wigner to a Poisson distribution. We remark that these probabilities distributions are universal since no fitting parameters are required once the plot is versus $s/\langle s \rangle$, where $\langle s \rangle = \int P(s) s ds$.

Since one cannot say, based on a finite sample, when one of the distributions becomes “exactly” Poisson or Wigner, one looks for the value of λ_{th} that makes both distributions “as different as possible from each other.” To do this we use (following ref. 16) the Jensen-Shannon (JS) divergence as a measure of the distance between two distributions. It is defined as

$$D_{JS}[P_1, P_2] = H[a_1 P_1 + a_2 P_2] - a_1 H[P_1] - a_2 H[P_2]. \quad (9)$$

$H[P] = -\sum_i P(s_i) \log P(s_i)$ is the Shannon entropy of the distribution P , and $a_1, a_2 = 1 - a_1$ are positive weights of each distribution. In what follows, we shall choose the weights as proportional to the support of the section of the (unfolded) spectrum considered to evaluate the level-spacing. This ensures that the JS divergence is

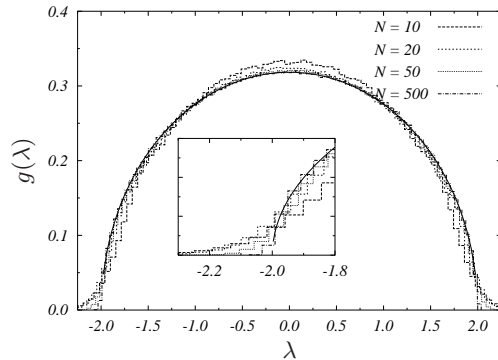


FIG. 3: DOS of GOE matrices at several N . The solid line is the semicircular law predicted at $N \rightarrow \infty$. Inset: zoom on the left tail.

not affected by differences in sizes [22]. The problem of finding the threshold is then reduced to finding the maximum of $D_{JS}[P_1, P_2]$ as function of λ_{th} . We stress that the ideas behind the method are justified only in the large N limit, and a study of finite-size effects is thus crucial in this context.

IV. RESULTS

A. A case study: the GOE

We have applied this procedure to the GOE, as a test and illustration of the method. We generated ensembles of $N \times N$ random matrices for $N = 10, 20, 50, 500$ with i.i.d. elements (taken from Gaussian distribution with zero mean and variance $1/\sqrt{N}$) and computed the DOS by numerical diagonalization (Fig. 3). The JS divergence has a maximum that tends to the band edge as N grows (Fig. 4, top), indicating that there is no localization threshold in this system, as it is known theoretically.

To gain further insight into the workings of the method, we have also tried fitting the level-spacing distribution restricted to eigenvalues lower than λ_{th} with the functions interpolating between Poisson and Wigner-Dyson, thus defining a kind of order parameter for localization (π in the case of the linear combination, Eq. 6, q in the case of the Brody distribution, Eq. 8). Both π and q should be zero if $\lambda_{th} \leq \lambda_L$ and non-zero otherwise. As Fig. 4 shows, both order parameters start from being different from their minimum at a value which roughly corresponds to the maximum of the JS divergence. However, the minimum value is not zero, most likely due to finite-size problems. Unfortunately, it is not possible to verify that in this case, because increasing N decreases the fraction of localized states such that their number remains finite even when $N \rightarrow \infty$ [19].

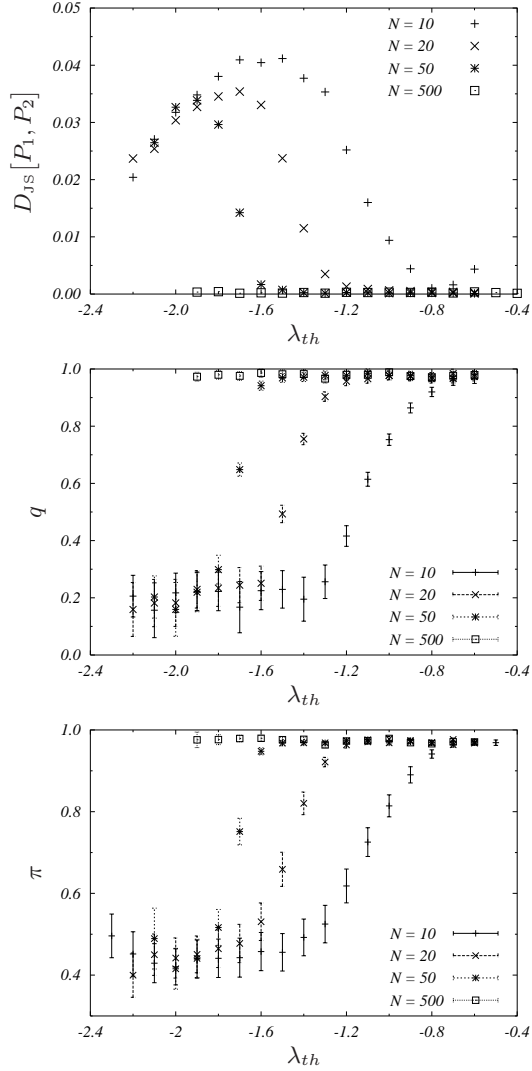


FIG. 4: Top: JS divergence for GOE matrices at different N . Middle: The Brody parameter (see text) for the same values of N . Bottom: The order parameter π from the linear approximation (6).

B. The INM spectrum

We have studied the soft-sphere binary mixture of ref. 24 at unit density and $T = 0.2029$ (to be compared with the mode-coupling critical temperature $T_c \approx 0.2262$). Equilibration of the supercooled liquid at this temperature has been possible thanks to the fast Monte Carlo algorithm of ref. 25. From the physical point of view, we are interested in studying the nature of negative modes (which represent about 4.3% of the total modes for this system). At the temperature considered, the dynamics is highly arrested, and diffusion events are rare (indeed, at the mean field level, such as mode-coupling theory, diffusion is completely suppressed below T_c). Accordingly, one expects that all or most of the negative modes correspond to localized eigenvectors (*i.e.* local re-

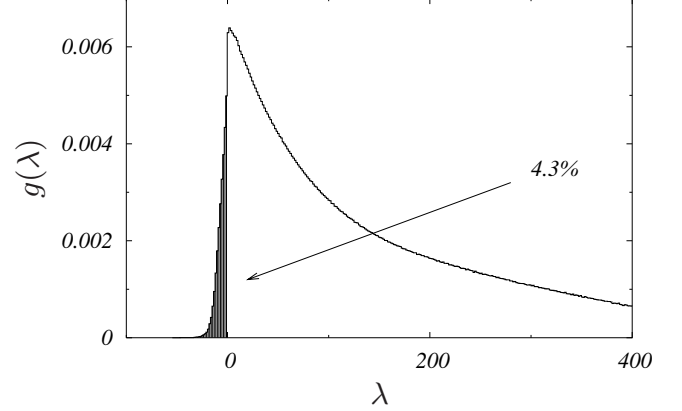


FIG. 5: INM spectrum of the binary mixture of soft spheres at $\Gamma = 1.49$ as obtained from 300 equilibrium configurations ($N = 2048$).

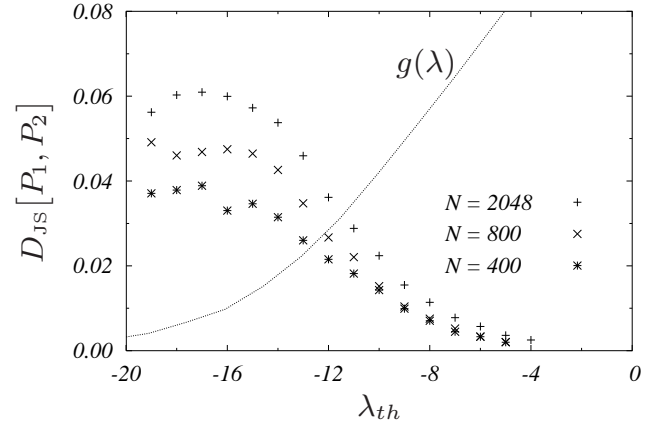


FIG. 6: The Jensen-Shannon divergence for the negative tail of the spectrum of Fig. 5. The DOS $g(\lambda)$ is also plotted (here it is normalized such that $\int_{-\infty}^0 g(\lambda) = 1$).

arrangement of a non extensive number of particles). We find that this is not the case.

In Fig. 5 we show the INM spectrum for a system of 2048 soft spheres. The spectrum is expected to have two localization thresholds (on the positive and negative tails), so to apply the scheme above we need first to separate the positive and negative modes. We focus on the negative modes. The JS divergence for the negative part, evaluated as explained above, is shown in Fig. 6 for $N = 400, 800$ and 2048 particles. As N increases, the maximum of these curves does not shift as in the GOE example but it becomes sharper, pointing to a localization threshold. A quadratic fit of the peak, for the largest size system leads to $\lambda_L = -16.8 \pm 1.4$. We also verify that the two distributions $P_1(s)$ and $P_2(s)$ are indeed Poisson and Wigner (respectively) for this threshold value.

We next try to fit with the linear interpolation: in

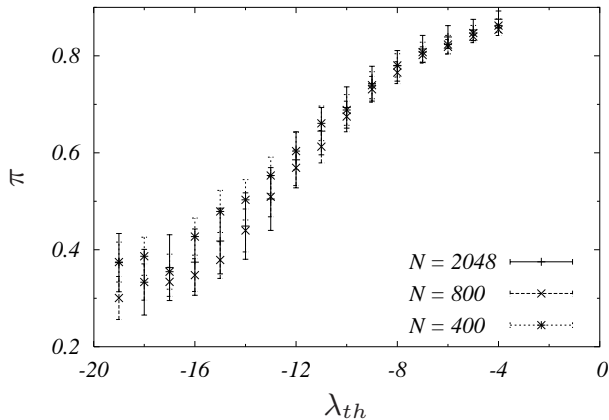


FIG. 7: The parameter π is found by fitting the level-spacing distribution $P(s|\lambda < \lambda_{th})$ to the form in (6).

Fig. 7 we plot the fitting parameter π (cf. Eq. 6) for the $P(s|\lambda < \lambda_{th})$. As in the GOE case, the parameter goes to a non-zero value. At the values of N available to us, there is no clear evidence that larger system sizes will make π go to zero for $\lambda_{th} \leq \lambda_L$. To check whether this behavior is an indication of some non-linear effect, we have performed the following test. Assuming that the threshold is actually at λ_L , for each of the values of λ_{th} of Fig. 7 we have generated random spacings distributed with the linear combination of Poisson and Wigner-Dyson. The weight π was taken as proportional to the number of actual levels between λ_L and λ_{th} , i.e.

$$\pi \propto \int_{\lambda_L}^{\lambda_{th}} g(\lambda) d\lambda.$$

We then tried the same fitting procedure we applied to the INM spectrum, to see whether it would yield the same π used. We found that samples of at least ≈ 90000 levels were needed in order to recover the correct weight with the fit (this is more than ten times greater than the number of levels available from the INM spectrum of the simulated liquid). Hence we attribute the finite value of π (Fig. 7) to finite-size effects.

In the fit with the Brody distribution, the finite-size effects seem to be less pronounced (see Fig. 8). The Brody parameter is consistent with a localized phase for $\lambda \lesssim -16$: here one can see that in the large N limit the order parameter goes to zero as $\lambda \leq \lambda_L$. So the results from the fits and from the JS divergence are consistent with the existence of a localization threshold.

Though a more accurate determination of the threshold needs larger system sizes, this results shows that most (more than 96%) of the negative modes in this system are of an extended nature.

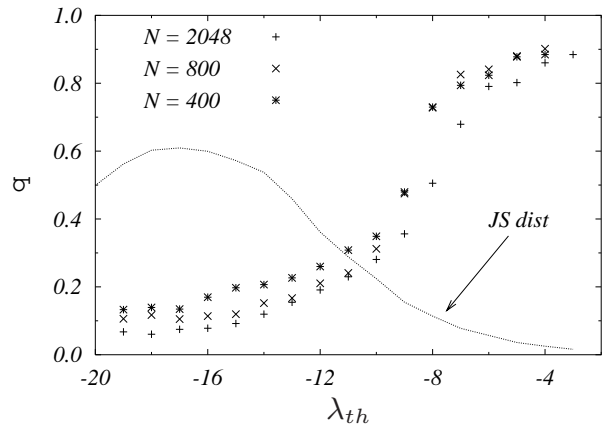


FIG. 8: The Brody order parameter for the supercooled liquid at different sizes.

V. CONCLUSIONS

The study of the level-spacing distribution of the INM spectrum of a glass forming liquid in the supercooled regime we have presented shows that it is possible to locate the mobility edge for the negative tail of this spectrum with reasonable precision (other techniques like the inverse participation ratio are usually less precise). The INM level-spacing distribution is reasonably described in terms of Wigner and Poisson distributions and this information can be used to determine the mobility edge.

We have applied the technique to the soft-spheres binary liquid below T_c . Our result can be summarized by stating that at this temperature only 3.4% of the negative modes are localized. This adds to the evidence (see e.g. the critique by Gezelter et al. [8]) that not all extended imaginary modes can be regarded as leading to free diffusion. It has been argued [2, 4, 5, 7] that not all extended negative modes should be considered unstable in the sense of this approach [one should exclude false saddles (also called shoulder modes) and saddles that do not connect different minima, an analysis we have not done here]. Our result implies not only that many negative modes cannot be regarded as diffusive (not surprising in view of earlier results, e.g. refs. 4, 8), but also that the vast majority of these non diffusive negative modes are extended, even below T_c .

It would be interesting to extend these results to study the temperature dependence of the localization properties of the INM across the Mode Coupling temperature. We expect to do this in the near future.

Acknowledgments

We thank G. Biroli, O. Bohigas, N. Deo, S. Franz, V. Martín-Mayor, G. Parisi and P. Verrocchio for useful discussions and comments. S.C. was supported by

the ECHP programme under contract HPRN-CT-2002-00307, *DYGLAGEMEM*. T.S.G. is a career scientist of

the Consejo Nacional de Investigaciones Científicas y Técnicas (CONICET, Argentina).

-
- [1] T. Keyes, J. Chem. Phys. **101**, 5081 (1994); J. Phys. Chem. A **101**, 2921 (1997).
 - [2] S. Bembenek and B. Laird, Phys. Rev. Lett. **74**, 936 (1995); J. Chem. Phys. **104**, 5199 (1996).
 - [3] F. Sciortino and P. Tartaglia, Phys. Rev. Lett. **78**, 2385 (1997).
 - [4] C. Donati, F. Sciortino, and P. Tartaglia, Phys. Rev. Lett. **85**, 1464 (2000).
 - [5] E. La Nave, A. Scala, F. W. Starr, F. Sciortino, and H. E. Stanley, Phys. Rev. Lett. **84**, 4605 (2000); E. La Nave, A. Scala, F. W. Starr, H. E. Stanley, and F. Sciortino, Phys. Rev. E **64**, 036102 (2001).
 - [6] S. Sastry, N. Deo, and S. Franz, Phys. Rev. E **64**, 016305 (2001).
 - [7] E. La Nave, H. E. Stanley, and F. Sciortino, Phys. Rev. Lett. **88**, 035501 (2002).
 - [8] J. D. Gezelter, E. Rabani, and B. J. Berne, J. Chem. Phys. **107**, 4618 (1997).
 - [9] T. Keyes, W.-X. Li, and U. Zurcher, J. Chem. Phys. **109**, 4693 (1998).
 - [10] P. A. Lee, T. V. Ramakrishnan, Rev. Mod. Phys. **57**, 287 (1985).
 - [11] P. W. Anderson, Phys. Rev. **109**, 1492 (1958); D. J. Thouless, Phys. Rep. **13**, 93 (1974); R. Abou-Chacra, D. J. Thouless, and P. W. Anderson, J. Phys. C **6**, 1734 (1973).
 - [12] P. Cizeau, J. P. Bouchaud, Phys. Rev. E **50**, 1810 (1994).
 - [13] M. Mézard, G. Parisi, and A. Zee, Nucl. Phys. B **559**, 689 (1999).
 - [14] S. Ciliberti, T. S. Grigera, V. Martin-Mayor, G. Parisi, and P. Verrocchio, cond-mat/0403122.
 - [15] R. J. Bell, P. Dean, Discuss. Faraday Soc. **50**, 55 (1970).
 - [16] P. Carpena and P. Bernaola-Galván, Phys. Rev. B **60**, 201 (1999).
 - [17] W. Götze and L. Sjogren, Rep. Prog. Phys. **55**, 241 (1992).
 - [18] T. Guhr, A. Müller-Groeling, and H. A. Weidenmüller, Phys. Rep. **299**, 189 (1998).
 - [19] M. L. Mehta, *Random Matrices* (Academic Press, New York, 1991).
 - [20] O. Bohigas, *Random Matrix Theory and Chaotic Dynamic*, in *Chaos and Quantum Physics*, M.J. Giannoni, A. Voros and J. Zinn-Justin eds, Elsevier Science Publisher B.V., (1991).
 - [21] See for example T.A. Brody, J. Flores, J.B. French, P.A. Mello, A. Pandey, and S.S.M. Wong, Rev. Mod. Phys. **53**, 385 (1983).
 - [22] P. Bernaola-Galván, R. Román-Roldán, and J. L. Oliver, Phys. Rev. E **53**, 5181 (1996).
 - [23] W. H. Press, S. A. Teukolsky, W. T. Vetterling, and B. P. Flannery, *Numerical Recipes*, Second Edition (Cambridge University Press, Cambridge, 1992), also at <http://www.library.cornell.edu/nr/bookcpdf.html>.
 - [24] B. Bernu, J.-P. Hansen, Y. Hiwatari, and G. Pastore, Phys. Rev. A **36**, 4891 (1987); J.-L. Barrat, N. Roux, and J.-P. Hansen, Chem. Phys. **149**, 197 (1990).
 - [25] T. S. Grigera and G. Parisi, Phys. Rev. E **63**, 045102(R) (2001).